

Optical properties of ultrarough silver films on silicon

Cite as: Journal of Applied Physics **80**, 1058 (1996); <https://doi.org/10.1063/1.362841>

Submitted: 08 January 1996 • Accepted: 16 April 1996 • Published Online: 04 June 1998

H. Neff, S. Henkel, J. K. Sass, et al.



View Online



Export Citation

ARTICLES YOU MAY BE INTERESTED IN

[Influence of postdeposition annealing on the structural and optical properties of sputtered zinc oxide film](#)

Journal of Applied Physics **80**, 1063 (1996); <https://doi.org/10.1063/1.362842>



Applied Physics
Reviews

Read. Cite. Publish. Repeat.

19.162
2020 IMPACT FACTOR*



Optical properties of ultrarough silver films on silicon

H. Neff

TZN Forschungs-und Entwicklungszentrum Unterlüss GmbH, Neuensothriether Strasse 20, D-29345 Unterlüss, Germany

S. Henkel

1. Physikalisches Institut der RWTH Aachen, D-52056 Aachen, Germany

J. K. Sass

Fritz Haber Institut der Max Planck Gesellschaft, Faradayweg 4-6, D-14195 Berlin- Dahlem, Germany

E. Steinbeiss, P. Ratz, J. Müller, and W. Michalke

Institut für Physikalische Hochtechnologie (IPHT), Helmholtzweg 4, D-007743 Jena, Germany

(Received 8 January 1996; accepted for publication 16 April 1996)

The optical properties of inhomogeneously grown rough silver films have been analyzed on the basis of reflectance measurements. Data have been recorded within the wave number range $50 \text{ cm}^{-1} < \lambda^{-1} < 50\,000 \text{ cm}^{-1}$. The results are compared with compact and fairly smooth films, made from the same metal. Rough films reveal very low reflectance and high absorptivity values of nearly 1, at wave numbers $>200 \text{ cm}^{-1}$. The reflectance of these films is peaking at the bulk plasma resonance $h\nu_p$ of silver at 3.87 eV. Smooth compact films, in contrast, show a pronounced minimum at the same energy. Based on an effective medium approach and available literature data, the dielectric function (DF) and absorption coefficient have been calculated. For rough films, the real part of the DF remains positive within the whole spectral range, but is negative for compact films below $h\nu_p$, in agreement with published data. The calculated DF of the inhomogeneously grown films fully resembles the experimental observations. © 1996 American Institute of Physics. [S0021-8979(96)06714-X]

I. INTRODUCTION

Optical absorbers with high efficiency are key components towards the fabrication of sensitive thermal radiation detectors. They usually are deposited as a thin layer on top of the heat sensitive element. Film thickness and material density are crucial quantities, since they account for the effective thermal mass and, hence, define thermal time constant and frequency range of operation of the device.

To establish sufficiently high optical absorptance and device performance appropriate selection of the absorber material is an important issue.¹ Under terrestrial conditions and in connection with phonon noise limited performance, thermal detectors successfully compete with quantum detectors only in the far IR regime² and wavelengths $\lambda > 12 \mu\text{m}$. Background limited superior performance (BLIP) is established, in contrast, under outer space conditions and at low T . Thus, only few materials meet the given requirements. Dielectrics typically fail, due to their relatively large optical band gaps and weak absorptivity in the far IR region. Metal films commonly are highly reflective when deposited as an homogeneous layer under high vacuum conditions. The solution is rough, inhomogeneously growing semimetallic or metallic films, where rigid optical boundary conditions are lifted through soft, poorly defined interfaces and surfaces. Under these conditions, optical reflectance values usually remain low. Examples are black gold and black carbon films.³ The surface of these materials appears optically black since its open, porous, and granular structure minimizes optical reflectance. Absorptivity values of nearly 100% are achievable for some wavelength regions. Under ideal conditions, the optical properties of these materials should not vary with

photon energy over the whole range of interest.

In this work, the optical properties of ultrarough or black silver films on silicon have been addressed, covering the wave number range $50 \text{ cm}^{-1} < \lambda^{-1} < 50\,000 \text{ cm}^{-1}$. The data, eventually, are compared with the behavior of the compact metal. Among the noble metals, silver displays a well defined plasma oscillation, where the free-electron system of the solid is collectively resonating. Within the quantum representation, these excitations are described as quasi-particles, i.e., plasmons. They usually are probed directly by electron loss spectroscopy (ELS), applied to compact thin films of the solid. To some degree, the many body excitation determines the dielectric function of the solid, and thus severely affects the optical properties of the material.

II. EXPERIMENT

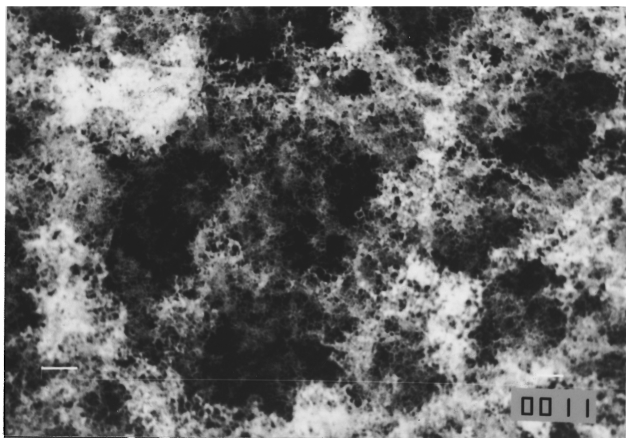
Briefly, rough silver films have been deposited onto polished Si(100) surfaces through evaporation of the metal in a N_2 or He atmosphere at a pressure of 1 mbar. Under these circumstances, the metal atoms coagulate from the gas phase into small sphericals. Upon their condensation onto the silicon surface, a fluffy network is formed at a density of 2%–5% of the compact solid. Film thickness is ranging from 5 to 7 μm , but is difficult to determine exactly. The film structure has been analyzed through transmission electron microscope (TEM), and scanning electron microscope (SEM) characterization. This is shown in Figs. 1(a) and 1(b). The TEM micrograph of Fig. 1(a) illustrates the formation of small clusters of metal atoms, where a very small amount of silver has been evaporated under identical conditions onto a thin carbon foil. The diameter of the primary particles is

transmission electron microscopy



(a) $\longleftarrow 0.1 \mu\text{m}$

scanning electron microscopy



(b) $\longleftarrow 1 \mu\text{m}$

FIG. 1. (a) TEM micrograph of isolated silver clusters, deposited onto an amorphous carbon foil. (b) SEM micrograph of the fluffy network, formed through coagulation of the particles on a silicon surface.

approximately 10 nm. The SEM micrograph at reduced magnification in Fig. 1(b) illustrates the microstructure of condensed rough films on silicon, forming the above-mentioned network. Compact films have been prepared through evaporation of the metal under high vacuum conditions. Optical reflectance data from the films have been recorded, using a Bruker 113 v Fourier spectrometer at wave numbers $<5000 \text{ cm}^{-1}$, while a LAMBDA2 spectrometer has been employed within the spectral region $9000 \text{ cm}^{-1} < \lambda^{-1} < 50\,000 \text{ cm}^{-1}$.

III. OPTICAL DATA ANALYSES

The dielectric function (DF) and absorption coefficients of the films eventually have been obtained from the optical measurements, in connection with a multilayer Fresnel calculation and an automated fitting routine to establish best

agreement. Data are compared with the behavior of smoothly grown films, deposited onto the same substrate material.

The fitting routines used for the calculations rely on an effective medium model, combined with a percolation approach. To establish the minimum deviation between measurements and calculated data, the above-mentioned fitting routine has been employed. The associated algorithm involves two steps. First, the macroscopic parameters like layer thickness, volume fraction, etc. have been determined by use of a parametrized spectral density function, establishing a set with the lowest error. Second, the spectral density has been fitted in detail. This has been achieved through small corrections to the spectral density, determined through the deviation and sensitivity of a given value of $g(n)$ to experimental data. A detailed description is given elsewhere.^{4,5}

Briefly, the dielectric function of a composite material, designed from two different phases with different complex dielectric functions, is written as

$$\epsilon(\mathbf{r}) = \begin{cases} \epsilon_1 & \text{if } \mathbf{r} \text{ is within phase 1} \\ \epsilon_2 & \text{if } \mathbf{r} \text{ is within phase 2.} \end{cases} \quad (1)$$

For the inhomogeneous films under study, one phase is taken as compact silver, where the appropriate DF has been taken from the literature. The second phase is treated as vacuum. The effective density of the resulting composite is only a few percent of the compact material.

From $\epsilon(r)$ an effective dielectric function ϵ_{eff} is defined, independent of r . Averaging over the volume V yields the relation

$$\frac{1}{2V} \epsilon_0 \int_V \epsilon(r) \mathbf{E}^2(\mathbf{r}) d\mathbf{r} = \frac{1}{2} \epsilon_0 \epsilon_{\text{eff}} \left(\frac{1}{V} \int_V \mathbf{E}(\mathbf{r}) d\mathbf{r} \right)^2. \quad (2)$$

This expression is convenient, provided that the volume contains a sufficiently large number of inhomogeneities and the electric-field E is nearly constant within V .

In other words, the characteristic length scale of the inhomogeneities, defined through the particle size or distance between them, should be much smaller than the wavelength of the incoming radiation. This condition is known as the electrostatic limit. To derive the effective dielectric constant ϵ_{eff} from Eq. (2), one expands ϵ_{eff} in terms of the geometrical electrostatic resonances of the given system. These resonances only come into effect, if the (generally complex) quotient ϵ_1/ϵ_2 becomes negative and real. To transform all resonances into a finite interval, ϵ_{eff} is replaced through the reduced dielectric constant, defined as

$$t = \frac{\epsilon_2}{\epsilon_2 - \epsilon_1} = t' + it''. \quad (3)$$

Especially for the case of multiple resonances that are expected if the system is statistically arranged, it is convenient to use an integral representation instead of a series expansion. This treatment is leading to an expression of the form known as the Bergman representation⁴

$$\epsilon_{\text{eff}} = \epsilon_2 \left(1 - f \int_0^1 \frac{g(n, f)}{t - n} dn \right), \quad (4)$$

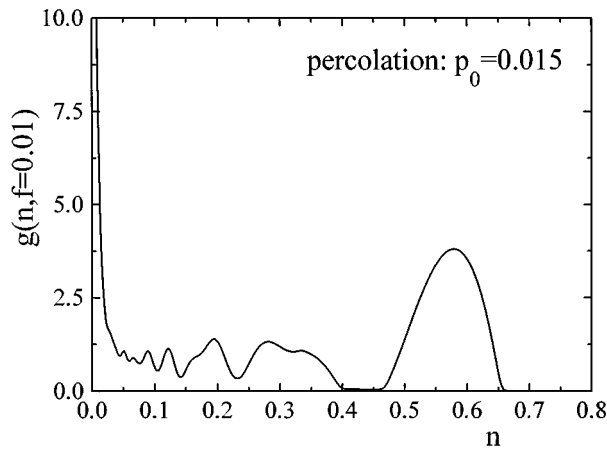


FIG. 2. Spectral density $g(n, f)$, obtained from the effective medium calculations. Density of the metallic fraction is 1%, the percolation factor is 0.015.

where f is the volume fraction, taken through phase 1.

Here the integration variable n is scanning all possible resonances. The spectral density $g(n, f)$ determines how strong they appear for the given microtopology. The actual calculations are performed in an automated fitting routine, until best agreement with the experimental data is established.

The material properties are related to the quantity t . The effects of geometry, hence, are solely assigned to f and the spectral density $g(n, f)$. Form and size of $g(n, f)$ are limited through the so-called momentum equation

$$\int_0^1 g(n, f) dn = 1 \quad (5)$$

and, if the effective medium is isotropic

$$\int_0^1 n \times g(n, f) dn = \frac{1-f}{3}. \quad (5)$$

The spectral density as a function of n , obtained for the present data from the iterative fitting procedure, is illustrated in Fig. 2. A fully consistent topological interpretation of the spectral function, however, remains somewhat delicate. The peak at $n=0.3$ would correspond to a resonating sphere. The strong peak at $n=0.55$ is correlated with the dip near $28\,000\text{ cm}^{-1}$, shown in the originally recorded reflectance spectrum and associated with the surface plasma resonance. Single silver clusters are not isolated particles, but cohere to each other. This behavior is treated through a further, percolation-type term applied to the spectral density, where p_0 determines the percolation strength.^{5,6} The spectral function then is given through

$$g(n, f) = p_0 \delta_r(n) + g_{\text{resid.}}(n, f), \quad (7)$$

where $\delta_r(n)$ represents the delta function.

IV. RESULTS AND DISCUSSION

Figs. 3(a), 3(b), and 4 display both the recorded and the fitted data for rough and smooth films. Data have been taken within the far infrared region at wave numbers 50

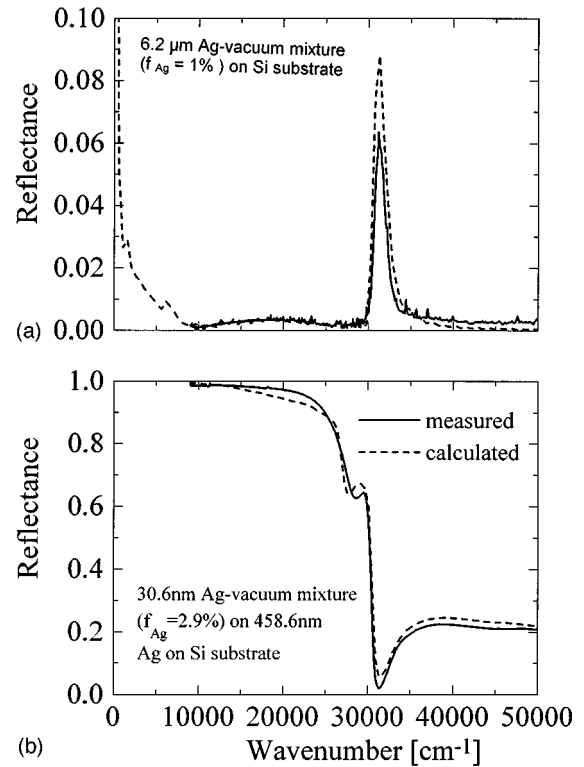


FIG. 3. Reflectance for the rough film [Fig. 3(a)] and the compact material [Fig. 3(b)] as a function of wave number. Experimental results are displayed through the solid line, fitted data correspond to the broken curves.

$\text{cm}^{-1} < \lambda^{-1} < 600\text{ cm}^{-1}$. The visible /UV regime has been addressed at values $9000\text{ cm}^{-1} < \lambda^{-1} < 50\,000\text{ cm}^{-1}$. Solid lines are experimental data. Broken lines are the result of the fitting procedure, taking into account the influence from the silicon substrate material. Reflectance values of rough films are remarkably low, but increase towards lower wave numbers, as indicated in Fig. 4, where the fitted data appear somewhat larger than the experimental values. In the visible and UV part of the spectra, a prominent peak is resolved that is located at $31\,300\text{ cm}^{-1}$ and photon energy $h\nu_p$ of 3.87 eV. Its position fully coincides with the bulk plasma resonance of

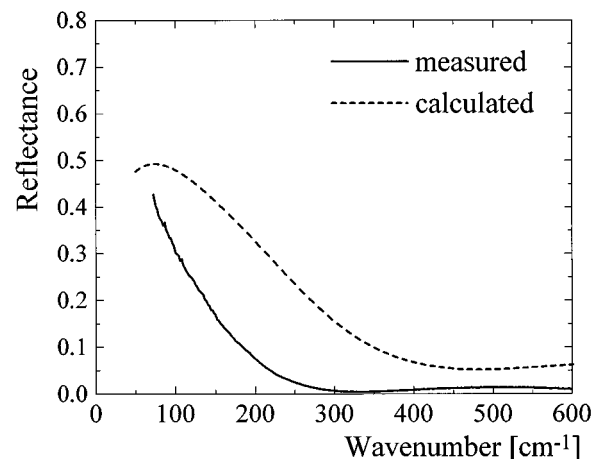


FIG. 4. Experimental (solid line) and fitted reflectance (dashed line) within the far infrared region for the inhomogeneously grown film.

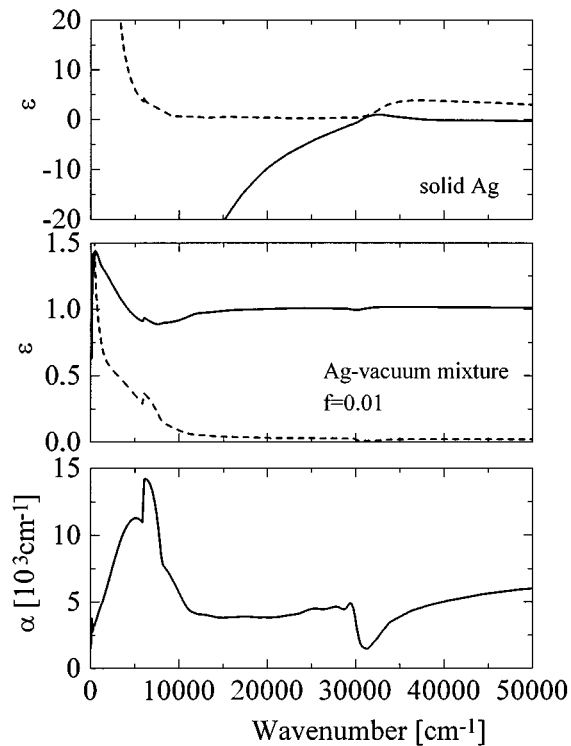


FIG. 5. Dielectric function of compact and inhomogeneously grown films for the visible UV region. The solid line is the real part, the broken line the imaginary part of the DF. Lower curve shows the calculated absorption coefficient of the rough film.

the silver.⁷ Note the presence of a further, rather broad maximum of reflectance near $20\,000\text{ cm}^{-1}$ and the minimum below the plasma resonance, resolved at $28\,000\text{ cm}^{-1}$. At this value (photon energy 3.47 eV), the position of the associated surface plasma resonance of silver is located.^{8,9}

Compact, rather smooth films reveal a remarkably different behavior. In agreement with published data, optical reflectance under these circumstances displays a pronounced dip, located precisely at the bulk plasma frequency of $31\,300\text{ cm}^{-1}$. Reflectivity increases to nearly 1 towards lower wave numbers, but retains at moderate values above the plasma frequency. The present compact silver films on silicon also consistently showed a swing near $29\,000\text{ cm}^{-1}$. It is related to the surface plasma resonance, placed slightly below the bulk plasma resonance. Its optical excitation requires the presence of nonperfect, slightly rough surfaces.⁹ This condition has been taken into account through a modified fitting procedure, where the surface roughness has been modeled through a further, thin rough adlayer placed on top of the compact smooth metal. Optical properties of this structure, again, have been fitted through a combination of the effective medium approach with published data of the DF for the dense material.^{10,11}

The results of the fitting procedures, applied to both rough and compact films, are illustrated below. The real (solid line) and imaginary part (broken line) of the DF and associated absorption coefficients (for the rough film) as a function of wave number are shown in Figs. 5 and 6. The

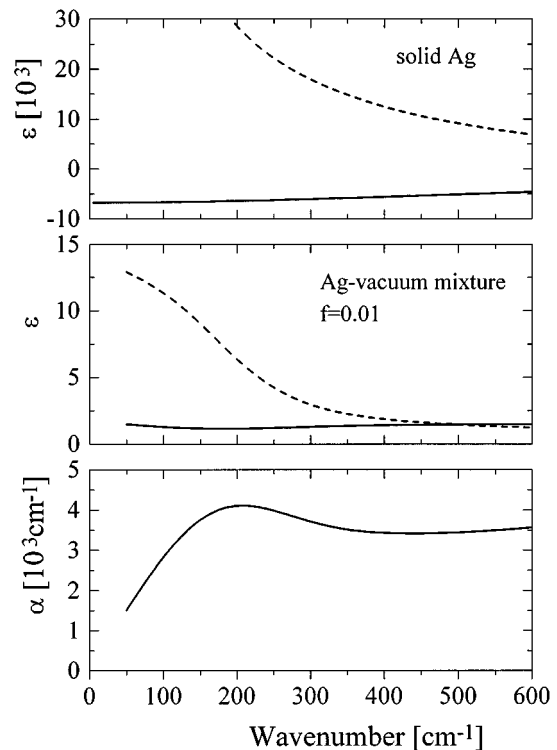


FIG. 6. Dielectric function of compact and inhomogeneously grown films for the far IR region. The solid line is the real part, the broken line the imaginary part of the DF. Lower curve shows the calculated absorption coefficient of the rough film.

related, thickness dependent optical absorbance of the rough film, finally, is displayed in Fig. 7.

There exist clear differences among the two materials systems. The real part of the dielectric function of rough films consistently remains positive within the full spectral regime. Its value near one well resembles vacuum conditions, as expected for the very low-density material under study. Variations appear at the bulk plasma resonance. Below $10\,000\text{ cm}^{-1}$, a distinct increase of both the real and imaginary part of the DF is observed. The latter result compares to the properties of compact films. The calculated optical absorbance is shown in Fig. 7.

Regarding future use of rough silver films as an optical absorber, the material under study would be considered as an acceptable solution, providing effective operation at wave numbers above 200 cm^{-1} . Again, absorptivity values of nearly 1 are achieved, depending on film thickness. Significant variations of the absorption coefficient only appear around the bulk plasma resonance, centered at $31\,300\text{ cm}^{-1}$, where changes of absorptivity around 30% have been resolved. In view of far infrared applications (FIRs) of the absorber films, the presence of the plasma resonance is without any consequences. Its use within the visible /UV region of the electromagnetic spectrum, however, would require properly selected optical filters to accommodate for the change of sensitivity.

The difference between inhomogeneously grown silver films and the compact phase, regarding their dielectric function, is remarkable. First of all, the real part of the dielectric

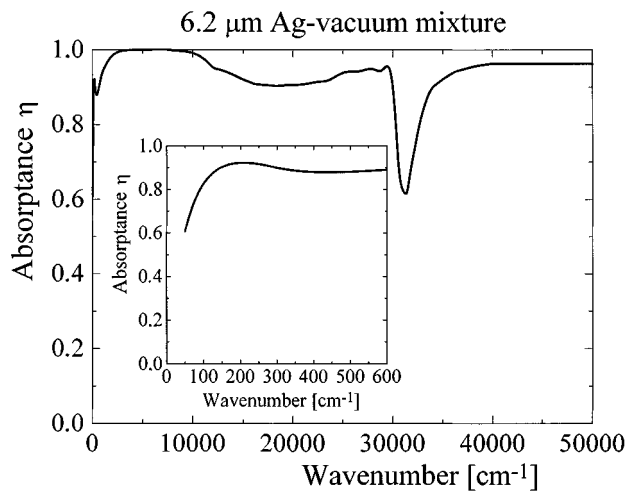


FIG. 7. Absorption coefficient of the rough film as a function of wave number. Inset shows the far IR region.

function of compact films, shown in Figs. 5 and 6, consistently remains negative at very large, increasing values for wave numbers below the plasma resonance. This agrees well with literature data. The imaginary part, in contrast, is small and increases to rather large positive values with decreasing wave numbers, as expected for a metallic conductor. Exactly at the bulk plasma resonance, the real part of the dielectric function disappears. Thin films at this energy therefore would appear transmitting. Reflectance and absorbance values at the resonance remain low. This behavior applies to all compact metals, exhibiting a well defined plasma resonance. To some degree, it also affects the properties of the inhomogeneously grown composite material under study.

To identify the origin of the prominent features of rough films shown in Fig. 3(a), the optical properties have been recalculated in absence of the silicon substrate. The result is illustrated in Fig. 8. Under these circumstances, the transmittance of a free standing layer of an inhomogeneously grown film would display a sharp peak at the bulk plasma resonance, a broad maximum around $18\,000\text{ cm}^{-1}$, and a minimum at $29\,000$ wave numbers. All features are in agreement with our experimental findings. The experimentally determined reflectance spectrum of the rough silver film under study, hence, is understood primarily as a result of backreflection of the incoming radiation from the silicon substrate. It thus is resembling the optical transmission characteristics of the metallic absorber.

V. CONCLUSIONS

In summary, the optical properties of thin inhomogeneously grown silver films have been evaluated, covering the far IR and visible/UV region of the electromagnetic spectrum. The material shows very small reflectance and high,

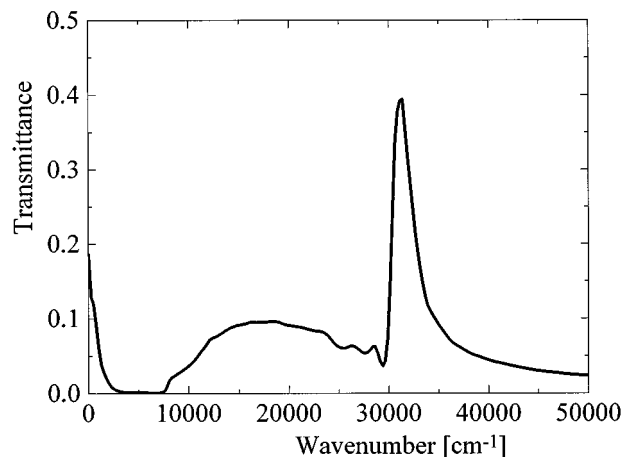


FIG. 8. Recalculated optical transmission for a free standing inhomogeneously grown film on the bases of the DF, displayed in Figs. 5 and 6.

nearly constant absorptivity values at wavelength $>50\ \mu\text{m}$. Within the UV range, the bulk plasma resonance accounts for strong variations of the absorbance near a photon energy of 3.87 eV . Based on an effective medium approach, the dielectric function and absorption coefficients α have been calculated from the experimental data. For rough films, the real part of the DF remains positive within the whole spectral range, but is negative for compact films below the plasma resonance, in agreement with published data. The observed peak of the reflectance of rough films at 3.87 eV is explained as a reflection of transmitted radiation from the substrate film interface. The high optical absorptivity of the prepared rough silver films is appropriate as an absorber material for broadband thermal radiation detectors.

¹W. Lang, K. Kahl, and H. Sandmeier, *Sens. Actuators A* **34**, 243 (1992).

²H. Neff, J. Laukemper, I. A. Khrebtov, A. D. Tkachenko, E. Steinbeiß, W. Michalke, M. Burnus, T. Heidenblut, G. Hefle, and B. Schwierzi, *Appl. Phys. Lett.* **66**, 2421 (1995).

³K. Mistl in *Absolute Radiometry* (Academic, New York, 1989), Chap. 2, p. 119.

⁴D. J. Bergman, *Phys. Rep. C* **43**, 377 (1978); S. Henkel, Ph.D. thesis, RWTH Aachen, 1995, ISBN 3-86073-277-3, and references cited therein.

⁵W. Theiß in *Festkörperprobleme/Advances in Solid State Physics* edited by R. Helbig (Vieweg, Braunschweig, 1993), Vol. 3, p. 149.

⁶T. Eickhoff, P. Grosse, S. Henkel, and W. Theiß, *Z. Phys. B* **88**, 17 (1992); E. Gorges, P. Grosse, J. Sturm, and W. Theiß, *ibid.* **B 94**, 223 (1994).

⁷See, for example, *Elementary Excitations in Solids*, edited by D. Pines (Benjamin, New York, 1963).

⁸R. A. Ferrell, *Phys. Rev.* **111**, 1214 (1958).

⁹H. Neff, J. K. Sass, and H. J. Lewerenz, *Surf. Sci.* **143**, L356 (1984) and references cited therein. At the metal-vacuum interface, for an ideal free electron system, the surface plasma resonance of silver would appear at $\omega_p/\sqrt{2}$ or $21\,000\text{ cm}^{-1}$. Since for silver, localized d states strongly affect the free electron system, the resonance is shifting to a value near $28\,000\text{ cm}^{-1}$.

¹⁰P. B. Johnson and R. W. Christy, *Phys. Rev. B* **6**, 4370 (1972).

¹¹D. E. Aspnes and A. A. Studna, *Phys. Rev. B* **27**, 985 (1983).